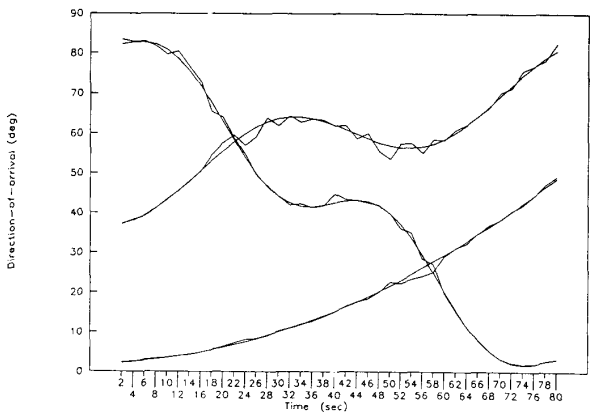

Fig. 2. $\sigma^2 = 10; N = 400$.

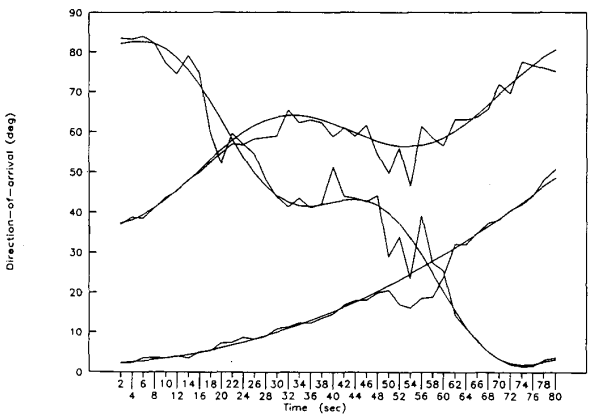

Fig. 3. $\sigma^2 = 50; N = 400$.

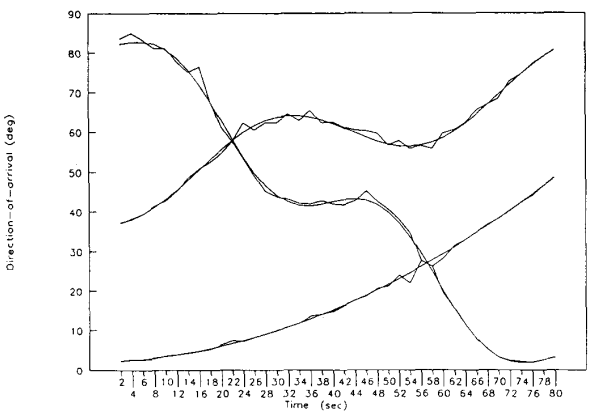

Fig. 4. $\sigma^2 = 50; N = 2000$.

a value of $\tau \geq 4$. The constants c_1 and c_2 are used to prevent too small gates, and c_3 is used to control the widths of the gates. In general, we can take $c_2 \geq c_1 \geq 1^\circ$ and $c_3 \geq 3$. In our simulation, we used $c_1 = 1^\circ, c_2 = 2^\circ$, and $c_3 = 4$. For different values of σ^2 and N, Figs. 1–4 give the true paths (smooth curves) and the estimated trajectories. For $N = 400$, Figs. 1–3 show the performance of the proposed algorithm for $\sigma^2 = 1, 10$, and 50, respectively. It is easily seen that the results are satisfactory for high and moderate SNR. Even if the SNR is as low as 1.76 dB ($\sigma^2 = 50$), the DOA are still well-tracked. [Note that $\mathrm{SNR} = 10\log(\mathrm{tr}\,\Gamma/\sigma^2)$.] From Fig. 4 it is seen that, for the same low SNR as in Fig. 3, when N increases to 2000, the tracking algorithm works better.

References

[1] Z. D. Bai, B. Q. Miao, and C. Radhakrishna Rao, "Estimation of direction of arrival of signals: Asymptotic results," in *Advances in Spectral Analysis and Array Processing*, vol. 11, S. Haykins, Ed., 1990, pp. 327–347.

[2] C. R. Sastry, E. W. Kamen, and M. Simaan, "An efficient algorithm for tracking and angles of arrival of moving objects," *IEEE Trans. Signal Processing*, vol. 39, no. 1, pp. 242–246, 1991.

[3] C. K. Sword, M. Simaan, and E. W. Kamen, "Multiple target angle tracking using sensor array outputs," *IEEE Trans. Aerospace, Electron. Syst.*, vol. 26, pp. 367–373, 1990.

A Generalized Null-Spectrum for Direction of Arrival Estimation

Jinho Choi, Iickho Song, Sangyoub Kim, and Yoon Kyoo Jhee

***Abstract*— A generalization of null-spectrum for the estimation of directions of arrival of signal sources is considered. The upper and lower bounds of a class of the generalized null-spectrum, the maximum and minimum null-spectra, are derived. We observe that the maximum null-spectrum has higher resolution capability than other null-spectra including the multiple signal classification and Min-Norm null-spectra. In addition, it is seen that the estimates of the direction of arrival obtained by using the maximum and multiple signal classification null-spectra have the same asymptotic distribution. Through computer simulation the probabilities of resolution of various null-spectra are obtained, from which we confirmed the resolution capability of the maximum null-spectrum.**

I. Introduction

For use in localizing narrow-band multiple signal sources, various eigenstructure-based null-spectra have been proposed in the literature (e.g., [1], [3], [4]). The eigenstructure-based null-spectra have a common feature of the subspace decomposition, i.e., the signal and noise subspaces can be decomposed using the eigenvalues of the covariance matrix of the array output. The two subspaces play an important role in estimating the directions of arrival (DOA's) of

Manuscript received October 15, 1991; revised February 17, 1993. The associate editor coordinating the review of this paper and approving it for publication was Prof. S. Unnikrishna Pillai. This research was supported by the Korea Science and Engineering Foundation (KOSEF) under Grant 921-0800-002-2 and by the Korea Advanced Institute of Science and Technology under an Internal Grant.

The authors are with the Department of Electrical Engineering, Korea Advanced Institute of Science and Technology (KAIST), Daejeon 305-701, Korea.

IEEE Log Number 9214183.

signals, as in the multiple signal classification (MUSIC) and the Min-Norm method.

Consider an L-element array whose output is $y(t) \in C^{L\times 1}$ with $C^{m\times n}$ the space of $m \times n$ complex-valued matrices, and assume the standard model of observation

$$y(t) = Ax(t) + n(t), \qquad t = 1, 2, \cdots, N. \tag{1}$$

In (1), it is assumed that the column vector $x(t)$ for M-signal sources is an $M \times 1$ zero-mean complex normal random vector and the additive noise $n(t)$ is a zero-mean complex normal random vector with covariance matrix σI. The full-rank covariance matrix of $x(t)$ is $E[x(t)x^H(t)] = R_x$, where E denotes the statistical expectation and H denotes the Hermitian transpose. The matrix $A = [a(\theta_1), a(\theta_2), \cdots, a(\theta_M)]$ is an $L \times M$ $(L > M)$ complex matrix, where θ_i is the DOA of the ith signal source. Here $a(\theta_i) \in C^{L\times 1}$ is called the steering vector. If we denote the covariance matrix of $y(t)$ by R_y, it is easy to see that

$$R_y = AR_xA^H + \sigma I. \tag{2}$$

The eigenvalues and eigenvectors of R_x are denoted by $\lambda_1 \geq \lambda_2 \geq \cdots \geq \lambda_L$ and $e_1, e_2, \cdots, e_L$, respectively, where $\lambda_{M+1} = \lambda_{M+2} = \cdots = \lambda_L = \sigma$. The ranges of the matrices $S \triangleq [e_1, e_2, \cdots, e_M]$ and $G \triangleq [e_{M+1}, e_{M+2}, \cdots, e_L]$ are called the signal and noise subspaces, respectively. We observe that $a^H(\theta)G = 0$ for $\theta \in \Theta$, where $\Theta \triangleq \{\theta_1, \theta_2, \cdots, \theta_M\}$, because the vectors $\{a(\theta_i), 1 \leq i \leq M\}$ are orthogonal to the noise subspace. If we define $D(\theta) = a^H(\theta)GG^Ha(\theta)$, the function $D(\theta)$ has zeros only at $\theta \in \Theta$ [5]. In practice, however, we can obtain only the estimates of S and G, $\hat{S}$ and $\hat{G}$, from the estimate of R_y, $\hat{R}_y = (1/N)\Sigma_{t=1}^{N} y(t)y^H(t)$. The MUSIC null-spectrum $f_{\mathrm{MU}}(\theta)$ is defined

$$f_{\mathrm{MU}}(\theta) = a^H(\theta)\hat{G}\hat{G}^Ha(\theta) \tag{3}$$

and is expected to have minimum points at around $\theta \in \Theta$. Therefore, we can estimate the DOA by taking the local minimum points of $f_{\mathrm{MU}}(\theta)$.

II. Constraint Equation for the Generalized Null-Spectrum

The estimates of the eigenvectors and the true eigenvectors can be related as

$$[S\vdots G] = [\hat{S}\vdots\hat{G}]P \tag{4}$$

where the perturbation matrix $P \in C^{L\times L}$ is of full rank. We can assume that the diagonal and off-diagonal elements of P are close to unity and zero, respectively, when the $\hat{e}_i$'s are faithful estimates of e_i's. The main motivation of this paper is that some information from the signal subspace S, in addition to that from the noise subspace G, can be of help in discriminating two closely located sources.

Let us partition the perturbation matrix P at the M th row and $(L - M)$th column, then we have

$$[S\vdots G] = [\hat{S}\vdots\hat{G}]\begin{pmatrix} P_{11} & P_{12} \\ P_{21} & P_{22} \end{pmatrix}$$

$$= [\hat{S}P_{11} + \hat{G}P_{21}\vdots\hat{S}P_{12} + \hat{G}P_{22}]. \tag{5}$$

Note that

$$P^HP = I. \tag{6}$$

Since range$\{A\}$ = range$\{S\}$, there exists a full-rank matrix $D \in C^{M\times M}$ that satisfies

$$S = AD \tag{7}$$

with which we have, for $\theta = \theta_k \in \Theta$

$$\begin{aligned} a(\theta_k) &= Au_k \\ &= Sw \\ &= [\hat{S}P_{11} + \hat{G}P_{21}]w \end{aligned} \tag{8}$$

where the elements of the vector u_k are zeros except for the kth element which is 1 and $w \triangleq D^{-1}u_k$. If we let $v_1 \triangleq P_{11}w$ and $v_2 \triangleq P_{21}w$, we have

$$v_1 = \hat{S}^Ha(\theta_k) = P_{11}w \tag{9}$$

and

$$v_2 = \hat{G}^Ha(\theta_k) = P_{21}w. \tag{10}$$

We can use P_{11} and P_{21} in estimating the DOA's because P_{11} and P_{21} depend on $a(\theta), \theta \in \Theta$, as can be seen from (9) and (10).

Since $P_{11} \simeq I$, we have from (9) and (10)

$$\hat{G}^Ha(\theta_k) \simeq P_{21}\hat{S}^Ha(\theta_k) \tag{11}$$

and

$$c \simeq a^H(\theta_k)\hat{S}P_{21}^HP_{21}\hat{S}^Ha(\theta_k) \tag{12}$$

where $c \triangleq a^H(\theta_k)\hat{G}\hat{G}^Ha(\theta_k)$. From (6), when $P_{11} \simeq I$, we have

$$P_{21}^HP_{21} \simeq B \triangleq \mathrm{diag}[\beta_1, \beta_2, \cdots, \beta_M]. \tag{13}$$

If we let $a^H(\theta_k)\hat{S} = [\alpha_1, \alpha_2, \cdots, \alpha_M]$, then (12) can be expressed as

$$c = \sum_{i=1}^{M} |\alpha_i|^2\beta_i. \tag{14}$$

Now let us consider the equation

$$\sum_{i=1}^{M} |\alpha_i(\theta)|^2\beta_i(\theta) = a^H(\theta)\hat{G}\hat{G}^Ha(\theta), \qquad \forall\theta \tag{15}$$

which is a generalization of (14) for all θ, where $\alpha_i(\theta)$ is the ith element of the row vector $a^H(\theta)\hat{S}$. We note that the value of $a^H(\theta)\hat{G}\hat{G}^Ha(\theta)$ for $\theta \in \Theta$ tends to be less than that for $\theta \notin \Theta$ when $\hat{G} \simeq G$. Note also that the value of $a^H(\theta)\hat{S}\hat{S}^Ha(\theta) = \Sigma_i|\alpha_i(\theta)|^2$ for $\theta \in \Theta$ tends to be greater than that for $\theta \notin \Theta$ when $\hat{S} \simeq S$. Therefore, the value of $\beta_i(\theta)$ for $\theta \in \Theta$ should be smaller than that for $\theta \notin \Theta$ in order to satisfy the constraint equation (15). This shows that a nonnegative weighted linear sum of $\beta_i(\theta), i = 1, 2, \cdots, M$, can be used as a null-spectrum for estimation of DOA's.

III. Generalized Null-Spectrum

Let us consider a hyperplane defined by

$$\begin{aligned} V(\theta) = \{\beta(\theta):\ & \sum_{i=1}^{M} |\alpha_i(\theta)|^2\beta_i(\theta) \\ & = a^H(\theta)\hat{G}\hat{G}^Ha(\theta), \beta_i(\theta) \geq 0\} \end{aligned} \tag{16}$$

where $\beta(\theta) = [\beta_1(\theta), \beta_2(\theta), \cdots, \beta_M(\theta)]^T$. Then, we define a generalized null-spectrum $f(\theta)$ as

$$f(\theta) = r^T(\theta)\beta(\theta), \qquad r(\theta) \geq 0 \quad \text{and} \quad \beta(\theta) \in V(\theta) \tag{17}$$

where $r(\theta) \geq 0$ implies that the elements of the vector r are all nonnegative. Since the weighting vector $r(\theta)$ determines the characteristics of the generalized null-spectrum, the determination of $r(\theta)$ is of high importance.

Property 1: Let $\hat{e}_i = e_i, i = 1, 2, \cdots, L$. If $\theta \in \Theta, \beta_i(\theta) = 0, i = 1, 2, \cdots, M$, and if $\theta \notin \Theta$, at least one $\beta_i(\theta)$ is positive.

Proof: If $\theta \in \Theta$ and $\hat{e}_i = e_i, i = 1, 2, \cdots, L$, we have $P_{11} = I, P_{21} = 0$, and $B = P_{21}^H P_{21} = \text{diag}[0, 0, \cdots, 0]$ from (5) and (13). Thus $\beta_i(\theta) = 0, i = 1, 2, \cdots, M$. If $\theta \notin \Theta$, we observe that $a^H(\theta)GG^Ha(\theta) \neq 0$, i.e., $a^H(\theta)GG^Ha(\theta) > 0$. Thus, from (16), there exists at least one $\beta_i(\theta) > 0$.

Property 1 implies that the generalized null-spectrum defined by (17) can be used to estimate DOA's, because the nonnegative function $f(\theta)$ has zeros only at $\theta \in \Theta$, when $e_i = \hat{e}_i, i = 1, 2, \cdots, L$.

Property 2: Suppose that $r(\theta) = r_{\text{MU}}(\theta) \triangleq [|\alpha_1(\theta)|^2, |\alpha_2(\theta)|^2, \cdots, |\alpha_M(\theta)|^2]^T$, which is nonnegative vector, then the generalized null-spectrum is the MUSIC null-spectrum.

We can show that any weighted MUSIC null-spectrum [5] $f_W(\theta) = a^H(\theta)\hat{G}W\hat{G}^Ha(\theta)$, where W is a positive semidefinite matrix (for which the Min-Norm null-spectrum [3] is a special case), is a generalized null-spectrum with $r(\theta) = r_W(\theta) \triangleq (f_W(\theta)/f_{\text{MU}}(\theta))r_{\text{MU}}(\theta)$.

Let us consider the following problems for the class of the generalized null-spectrum for which $r(\theta) = [1, 1, \cdots, 1]^T$.

Maximization Problem

$$\max\left\{\sum_{i=1}^{M}\beta_i(\theta)\right\}$$

$$\text{subject to } \beta(\theta) \in V(\theta)$$

Minimization Problem

$$\min\left\{\sum_{i=1}^{M}\beta_i(\theta)\right\}$$

$$\text{subject to } \beta(\theta) \in V(\theta)$$

If we denote by $f_{\max}(\theta)$ and $f_{\min}(\theta)$ the object functions of the *maximization* and *minimization problems*, respectively, then we have

$$f_{\max}(\theta) = \frac{a^H(\theta)\hat{G}\hat{G}^Ha(\theta)}{\min_{i\le i\le M}|\alpha_i(\theta)|^2} \tag{18}$$

and

$$f_{\min}(\theta) = \frac{a^H(\theta)\hat{G}\hat{G}^Ha(\theta)}{\max_{1\le i\le M}|\alpha_i(\theta)|^2}. \tag{19}$$

From (14), the null-spectra $f_{\max}(\theta)$ and $f_{\min}(\theta)$ are approximations of the Frobenius norm (F-norm) of the matrix P_{21} which satisfies the constraint equation (15). That is, $f_{\max}(\theta)$ and $f_{\min}(\theta)$ are obtained by maximizing and minimizing the matrix $||P_{21}||_F$, respectively, where $||.||_F$ is the Frobenius norm.

Now let us consider a normalization of the generalized null-spectrum which is defined by

$$\overline{f}(\theta) = \frac{f(\theta)}{||r(\theta)||_1} \tag{20}$$

where $||.||_1$ is the 1-norm. Then we have $\overline{f}_{\max}(\theta) = f_{\max}(\theta)$, and $\overline{f}_{\min}(\theta) = f_{\min}(\theta)$, and we note that $\overline{f}_{\text{MU}}(\theta) \neq sf_{\text{MU}}(\theta), -\pi \le \theta \le \pi$, for any constant s. It is interesting to see that the normalized weighted MUSIC null-spectrum, $\overline{f}_W(\theta)$, is independent of the positive semidefinite matrix W, i.e., $\overline{f}_{\text{MU}}(\theta) = \overline{f}_W(\theta)$ for any positive semidefinite matrix W. In addition, for some constant ϵ in [0, 1], the null-spectrum $f_\epsilon(\theta) = \epsilon f_{\min}(\theta) + (1-\epsilon)f_{\max}(\theta)$ is also a generalized null-spectrum. It is easy to see that $\overline{f}_\epsilon(\theta) = f_\epsilon(\theta)$.

IV. Resolution Capability of the Generalized Null-Spectrum

We now consider the resolution capability of the maximum and minimum null-spectra. Let us define the inverse null-spectra as

$$g_k(\theta) = \frac{||a^H(\theta)\hat{e}_k||^2}{||a^H(\theta)\hat{G}||^2} = \frac{h_k(\theta)}{f_{\text{MU}}(\theta)}, \quad k = 1, 2, \cdots, M \tag{21}$$

where $h_k\theta \triangleq ||a^H(\theta)\hat{e}_k||^2$. It is noteworthy that $f_{\max}(\theta) = \max_k\{1/g_k(\theta)\}$ and $f_{\min}(\theta) = \min_k\{1/g_k(\theta)\}$. We assume that the number of the signal sources is 2 and the DOA's of the two signal sources are quite close to each other, i.e., $\theta_1 \simeq \theta_2$.

First, when θ is close to the middle $\theta_m = \frac{1}{2}(\theta_1 + \theta_2)$ of the two DOA's, we have

$$a(\theta) \simeq a(\theta_m) + (\theta - \theta_m)d^H(\theta_m) \tag{22}$$

where $d(\theta) = da(\theta)/d\theta$. If we define

$$V_m = a^H(\theta_m)\hat{G}\hat{G}^Ha(\theta_m) \tag{23}$$

it is expected that

$$V_m \simeq a^H(\theta)\hat{G}\hat{G}^Ha(\theta), \qquad \text{for } \theta \simeq \theta_m. \tag{24}$$

From (21) we have

$$\begin{aligned} g_i(\theta) &\simeq \frac{1}{V_m}||(a(\theta_m) + (\theta - \theta_m)d(\theta_m))^H\hat{e}_i||^2 \\ &= \frac{1}{V_m}[h_i(\theta_m) + c_1(i)(\theta - \theta_m) + c_2(i)(\theta - \theta_m)^2] \end{aligned} \tag{25}$$

where

$$c_1(i) = 2\text{re}\{d^H(\theta_m)\hat{e}_i\hat{e}_i^Ha(\theta_m)\} \tag{26}$$

and

$$c_2(i) = ||d^H(\theta_m)\hat{e}_i||^2. \tag{27}$$

It is easy to see that if $c_1(i)$ is much smaller than $c_2(i)$, the function $g_i(\theta)$ has its minimum point at $\theta \simeq \theta_m$. Therefore, if we choose $g_i(\theta)$ for which $||a^H(\theta)\hat{e}_i||^2 = \min\{||a^H(\theta)\hat{e}_k||^2, k = 1, 2\}$, then only $g_i(\theta)$ can have a local minimum point around θ_m, since $||a^H(\theta)\hat{e}_i||^2 \ll ||a^H(\theta)\hat{e}_k||^2$ for $k \neq i$ [2]. This implies that the maximum null-spectrum can have a local minimum around θ_m.

Next, taking the derivatives of $g_i(\theta)$ with respect to θ, we have

$$\begin{aligned} g_i'(\theta) &= \frac{dg_i(\theta)}{d\theta} \\ &= [h_i'(\theta)f_{\text{MU}}(\theta) - h_i(\theta)f_{\text{MU}}(\theta)]/f_{\text{MU}}^2(\theta) \end{aligned} \tag{28}$$

and

$$\begin{aligned} g_i''(\theta) = [&h_i(\theta)(2f_{\text{MU}}''(\theta)f_{\text{MU}}'(\theta) - f_{\text{MU}}(\theta)f_{\text{MU}}(\theta)) \\ &- 2h_i'(\theta)f_{\text{MU}}(\theta)f_{\text{MU}}'(\theta) + h_i''(\theta)f_{\text{MU}}^2(\theta)]/f_{\text{MU}}^3(\theta). \end{aligned} \tag{29}$$

Let $g_i'(\hat{\theta}) = 0$ or $h_i'(\hat{\theta})f_{\text{MU}}(\hat{\theta}) = h_i(\hat{\theta})f_{\text{MU}}'(\hat{\theta})$, then $\hat{\theta}$ is expected to be close to θ_1 or θ_2. From (29), a sufficient condition for $g_i(\theta)$ to have a local maximum at $\theta = \hat{\theta}$ is $h_i''(\hat{\theta})f_{\text{MU}}(\hat{\theta}) < h_i(\hat{\theta})f_{\text{MU}}''(\hat{\theta})$. Thus, if $f_{\text{MU}}(\hat{\theta}) \simeq f_{\text{MU}}(\theta_i) = 0$, we have local maxima at $\theta = \theta_1$ and θ_2.

In summary, the maximum null-spectrum can have a local minimum around $\theta = \theta_m$ and local maxima around θ_1 and θ_2. This implies that we can discriminate two closely-located sources with the maximum null-spectrum.

Let us explain by geometrical interpretation why the maximum null-spectrum has higher resolution capability than other null-spectra. Since the numerators of the maximum, minimum, and MUSIC

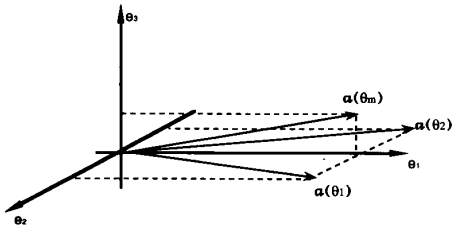

Fig. 1. Geometrical interpretation of the maximum null-spectrum.

null-spectra are all the same, it is easy to conceive that the high-resolution capability of the maximum null-spectrum comes out of the denominator, $\min_i |\alpha_i(\theta)|^2 = \min_i |a^H(\theta)\hat{e}_i|^2$. If $\hat{e}_i = e_i, i = 1, 2, \cdots, M$, the value of $|\alpha_i(\theta)|^2$ for $\theta \in \Theta$ is greater than that for $\theta \notin \Theta$, implying that the term $|\alpha_i(\theta)|^2$ contains some source localization information. Let us next consider Fig. 1 to see why the maximum null-spectrum has higher resolution capability than the minimum null-spectrum although they both have the term $|\alpha_i(\theta)|^2$ in the denominator. In Fig. 1, it is assumed that $L = 3$ and $M = 2$ with the DOA's being closely-located. Assuming that $\lambda_1 \geq \lambda_2 > \lambda_3 = \sigma$, it is easy to see in Fig. 1 that the signal subspace is span$\{e_1, e_2\}$ and the noise subspace is span$\{e_3\}$, and that the inner product of $a(\theta_1)$ (or $a(\theta_2)$) and e_1 is larger than that of $a(\theta_1)$ (or $a(\theta_2)$) and e_2. Under the assumption that the two DOA's are close, the projection of $a(\theta_m), \theta_m = \frac{1}{2}(\theta_1 + \theta_2)$, onto e_1 is larger than that onto e_3. Noting that $e_2 \propto a(\theta_1) - a(\theta_2)$ [2] and that e_1 resides between $a(\theta_1)$ and $a(\theta_2)$ since $e_1 \propto a(\theta_1) + a(\theta_2)$, the inner product of $a(\theta_m)$ and e_2 is approximately zero, while that of $a(\theta_m)$ and e_1 does not differ very much from the inner product of $a(\theta_1)$ (or $a(\theta_2)$) and e_1. Thus, the inner product of $a(\theta)$ and e_2 is more sensitive than that of $a(\theta)$ and e_1 to the change of θ around θ_1 and θ_2. From this geometrical interpretation, we can conclude that the minimum of $\alpha_i(\theta) = |a^H(\theta)\hat{e}_i|^2$ is the most sensitive one to the change of θ when the difference of DOA's is small. This is an intuitive explanation of the reason why the maximum null-spectrum has higher resolution capability than the other null-spectra. As is shown in Section VI, the maximum null-spectrum has an excellent resolution capability, which we believe is a result from using both the signal and noise subspaces.

V. A Statistical Property of the Generalized Null-Spectrum

In this section we consider a statistical property of the estimate of the DOA's when we use the generalized null-spectrum.

Theorem 1: The estimates of DOA's using the normalized null-spectra, $\overline{f}_{\max}(\theta), \overline{f}_{\min}(\theta), \overline{f}_{\mathrm{MU}}(\theta)$, and the MUSIC null-spectrum, $f_{\mathrm{MU}}(\theta)$, all have the same asymptotic distribution.

Theorem 1 can be proved using (18)–(20) and that all $r(\theta)$'s for the above null-spectra satisfy the regularity condition [5]. Theorem 1 implies that at least for asymptotic case $N \to \infty$, the mean square errors of the estimates of the DOA's are the same when we use the maximum and MUSIC null-spectra.

VI. Simulation Results

Let us consider a uniform array with sensor spacing half the wavelength of signal, assuming that the signal sources are uncorrelated. When $L = 10, M = 2, \theta_1 = 15°$, and $\theta_2 = 17°$, and SNR is 20 dB, the inverses of the normalized MUSIC, maximum, and minimum null-spectra are shown in Fig. 2. A sample covariance matrix is generated based on $N = 100$ independent data snapshots. The signal and additive noise are assumed to be white normal random variables. For the normalized MUSIC and minimum null-spectra, we can see

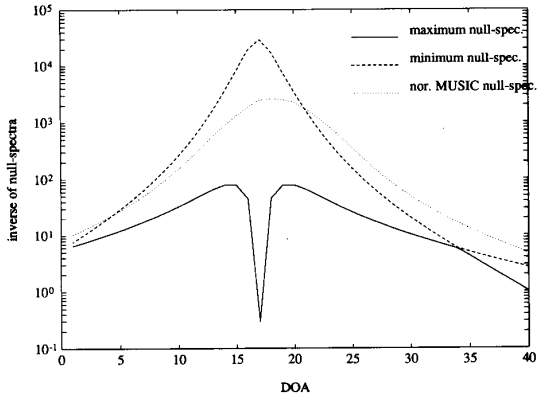

Fig. 2. An illustration of the various null-spectra when $N = 100, L = 10, M = 2 (\theta_1 = 15°$ and $\theta_2 = 17°)$, and SNR = 20 dB (average of five simulations).

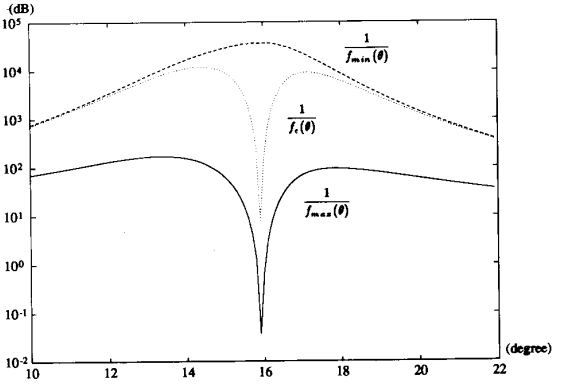

Fig. 3. A linear combination of the maximum and minimum null-spectra, $f_\epsilon(\theta)$, when $N = 100, L = 10, M = 2 (\theta_1 = 15°$ and $\theta_2 = 17°)$, and SNR = 20 dB.

only one peak between 15° and 17°; on the contrary, the inverse of the maximum null-spectrum have two peaks around 15° and 17°.

It is noteworthy that the two peaks of the maximum null-spectrum in Fig. 2 do not occur at exactly 15° and 17°. We can obtain unbiased DOA's using $f_\epsilon(\theta)$: however, it is not easy to determine the nonnegative constant ϵ or the nonnegative function $\epsilon(\theta)$ that is bounded, $0 \leq \epsilon(\theta) \leq 1$, and for which $f_\epsilon(\theta)$ gives us two unbiased DOA's. As an attempt to reduce the bias error, we considered the inverse of the null-spectrum $f_\epsilon(\theta)$ as shown in Fig. 3, for which $\epsilon = \inf(f_{\max}(\theta))/\{\inf(f_{\max}(\theta)) + \inf(f_{\min}(\theta))\}$.

To show the resolution performance of various null-spectra for the two closely-located signal sources we show the probability of resolution (PR) [2] versus SNR in Fig. 4. Each curve in Fig. 4 was obtained at intervals of 2 dB and each point was obtained from 500 trials. The well-known advantage of the Min-Norm over the MUSIC for a linear array can be seen. In addition, we observe that the resolution capability of the maximum null-spectrum based on the PR criterion is superior to that of the other null-spectra considered here: the curve of the maximum null-spectrum is about 20–30 dB lower than those of the other null-spectra, implying that the maximum null-spectrum has higher resolution capability than the others. The curves of the normalized MUSIC, the standard MUSIC, and the minimum null-spectrum almost coincide, which implies that the resolution capability of these three null-spectra are not quite different from each other under the PR criterion.

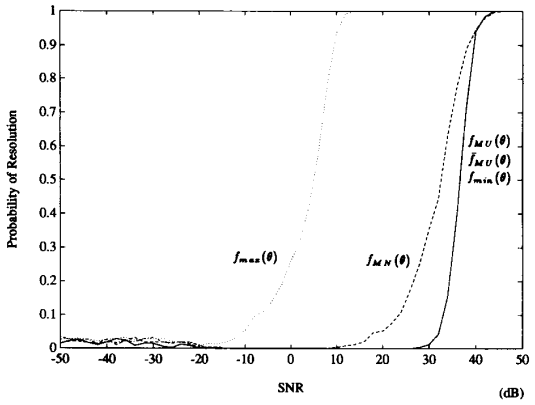

Fig. 4. Curves of probability of resolution versus SNR (in dB) for various null-spectra, $f_{\mathrm{MU}}(\theta), f_{\mathrm{MN}}(\theta), \bar{f}_{\mathrm{MU}}(\theta), f_{\min}(\theta)$, and $f_{\max}(\theta)$, when $N = 100, L = 10, M = 2\,(\theta_1 = 15^\circ$ and $\theta_2 = 17^\circ$. Each curve was obtained at interval of 2 dB and each point was obtained from 500 trials).

VII. Summary

Using a perturbation matrix, we introduced a hyperplane used to define a generalized null-spectrum, based on both the signal and noise subspaces, while the MUSIC and Min-Norm null-spectra are defined based only on the noise subspace. With the generalized null-spectrum, we derived the upper and lower bounds of a class of the generalized null-spectrum, called the maximum and minimum null-spectra, respectively. From a brief analysis of a class of the generalized null-spectrum and a geometrical interpretation, we expected that the resolution capability of the maximum null-spectrum would be superior to that of other null-spectra. By computer simulation it is shown that the maximum null-spectrum has higher resolution capability than other null-spectra. In addition, it is seen that the asymptotic distributions of the estimates of the direction of arrival by using the maximum and multiple signal classification null-spectra are the same.

References

[1] K. M. Buckley and X. L. Xu, "Spatial-spectrum estimation in a location sector," *IEEE Trans. Acoust., Speech, Signal Processing*, vol. 38, pp. 1842–1852, Nov. 1990.

[2] M. Kaveh and A. J. Barabell, "The statistical performance of the MUSIC and the Minimum-Norm algorithms in resolving plane waves in noise," *IEEE Trans. Acoust., Speech, Signal Processing*, vol. ASSP-34, pp. 331–341, Apr. 1986.

[3] R. Kumaresan and D. W. Tufts, "Estimating the angles of arrival of multiple plane waves," *IEEE Trans. Aero. Elect. Syst.*, vol. AES-19, pp. 134–139, Jan. 1983.

[4] R. O. Schmidt, "Multiple emitter location and signal parameter estimation," *IEEE Trans. Ant., Propagat.*, vol. AP-34, pp. 276–280, Mar. 1986.

[5] P. Stoica and A. Nehorai, "MUSIC, maximum likelihood, and Cramer-Rao bound," *IEEE Trans. Acoust., Speech, Signal Processing*, vol. 37, pp. 720–740, May 1989.

Computation of a Useful Cramer-Rao Bound for Multichannel ARMA Parameter Estimation

Mrityunjoy Chakraborty and Surendra Prasad

***Abstract*—It has been shown earlier that the problem of multichannel autoregressive moving average (ARMA) parameter estimation can be tackled in a computationally efficient way by converting the given process into an equivalent scalar, periodic ARMA process. This correspondence presents methods to compute the Cramer-Rao bound associated with the identification of the scalar ARMA equivalent of a given multichannel ARMA process. The elements of matrix are obtained by a few very simple operations like periodic AR filtering of certain downsampled versions of the input and output sequences and then cross-correlating the filter outputs. The filter is easily obtainable from the model equation and is common for all the parameters.**

I. Introduction

Autoregressive moving average (ARMA) models have found wide applications in various signal-processing applications like system identification, speech processing, spectrum estimation, etc. While the single-channel ARMA estimation can be extended to the multichannel case in a straightforward manner, the resulting alogrithms, however, employ extensive matrix operations such as inversion and Cholesky factorization and thus become computationally unattractive specially from real-time application point of view. This problem has been considered in [1] where the given multichannel ARMA process is converted into an equivalent scalar, periodic ARMA process. The corresponding estimation algorithms require scalar operations only and are well-suited for implementation on a pipelined processor. In [2], the scalar representation of the multichannel ARMA process has been used to develop fast adaptive least-squares lattice algorithms for the online identification of multichannel ARMA systems. A similar representation for a multichannel autoregressive (AR) process had earlier been derived by Pagano in [3] and identification algorithms based on this had been discussed in [4], [5].

The performance of these algorithms can be evaluated by computing the Cramer-Rao lower bound (CRLB) on the error covariance matrices of the parameters to be estimated. The error variance associated with any estimation technique that produces unbiased estimates of the parameters can be compared with the CRLB to obtain a measure of the estimation accuracy of that technique. In this correspondence, we present a method to compute the CRLB associated with the estimation of the scalar, periodic ARMA equivalent of a multichannel ARMA process. The derivation is based on the approach followed by Friedlander [6] for a single channel, stationary ARMA process. We show here that the elements of matrix (the CRLB is given by its inverse), for the scalar, periodic ARMA model under consideration, can be obtained by a few very simple operations. These involve constructing certain sequences by delaying and downsampling the scalar input and output sequences, filtering them by a periodic AR filter and cross-correlating the filter outputs. The filter is easily obtainable from the model equation and the same filter is employed for evaluating all the CRLB's.

Manuscript received April 17, 1992; revised July 8, 1993. The associate editor coordinating the review of this paper and approving it for publication was Prof. John Goutsias.

The authors are with the Department of Electrical Engineering, Indian Institute of Technology, New Delhi, India.

IEEE Log Number 9214186.